Pharmacology & Pharmacy, 2015, 6, 363-373
Published Online August 2015 in SciRes. http://www.scirp.org/journal/pp
http://dx.doi.org/10.4236/pp.2015.68037

Investigation of *in Vitro* and *in Vivo* Metabolism of Schisandrin B from Schisandrae Fructus by Liquid Chromatography Coupled Electrospray Ionization Tandem Mass Spectrometry

Tianxiu Qian[1,2], Pou Kuan Leong[3], Kam Ming Ko[3], Wan Chan[1*]

[1]Department of Chemistry, The Hong Kong University of Science and Technology, Hong Kong SAR, China
[2]Institute of Medicinal Plant Development, Chinese Academy of Medical Sciences & Peking Union Medical College, Beijing, China
[3]Division of Life Science, The Hong Kong University of Science and Technology, Hong Kong SAR, China
Email: *chanwan@ust.hk

Received 26 July 2015; accepted 21 August 2015; published 24 August 2015

Abstract

Schisandrin B (Sch B) is one of the active dibenzocyclooctadiene lignans found in the Schisandrae Fructus. Experimental studies have shown that Sch B possesses various pharmacological properties, including anti-cancer, neuroprotective and nephroprotective activities. However, no detailed information on its biotransformation was reported in the literature. Here, we investigated the *in vitro* and *in vivo* metabolism of Sch B by using ultra-performance liquid chromatography coupled with tandem mass spectrometry. *In vitro* study detected and identified one oxygenated metabolite. Four metabolites were detected and identified from the *in vivo* study. The results indicated that the metabolism of Sch B mainly involved the demethylation of methoxy groups, the opening of five-member ring and the glucuronidation of metabolites in rats. The metabolites were identified for the first time by MS/MS analyses.

Keywords

Schisandrin B, Metabolism, Disposition, UPLC-MS/MS

*Corresponding author.

How to cite this paper: Qian, T.X., Leong, P.K., Ko, K.M. and Chan, W. (2015) Investigation of *in Vitro* and *in Vivo* Metabolism of Schisandrin B from Schisandrae Fructus by Liquid Chromatography Coupled Electrospray Ionization Tandem Mass Spectrometry. *Pharmacology & Pharmacy*, **6**, 363-373. http://dx.doi.org/10.4236/pp.2015.68037

1. Introduction

Schisandrin B (Sch B, **Figure 1**) is the most abundant active dibenzocyclooctadiene lignan isolated from Schisandrae Fructus, the fruit of *Schisandra chinensis* (Turcz) Baillon (Wu-Wei-Zi in Chinese), which grows wild in Russia, Northeast China, Korea and Japan. The herb is commonly used in Chinese medicine for therapeutic (clinically prescribed for the treatment of viral and chemical hepatitis [1]) and health-promoting purposes. Given the broad range of therapeutic application of Schisandrae Fructus, scientists have attempted to isolate the active ingredient in Schisandrae Fructus. In 1950s, an active principle, schisandrin (a dibenzocyclooctadiene lignan) was first successfully isolated in form of crystal [2]. Then more than 30 lignans have been subsequently isolated, including Sch B. A growing body of experimental evidence has shown that Sch B possesses a wide spectrum of biological activities. It has been demonstrated that Sch B produces anti-cancer action *in vitro* and *in vivo* by inhibiting cancer invasion and metastasis or enhancing doxorubicin-induced apoptosis of cancer cells [3]-[6]. Sch B was also found to protect against carbon tetrachloride-induced hepatotoxicity [7]-[11] and enhance the hepatoprotection against various toxicants in rodents [12]-[16]. In addition, a number of studies showed that Sch B protected against nephrotoxicity induced by cisplatin [17] [18], cyclosporine A [19], gentamicin [20] and mercury in rodents [21] [22]. Other biological activities of Sch B included antioxidation [23]-[27], anti-inflammation [28] [29] and cytoprotection *in vitro* [30].

Lee *et al.* demonstrated that Sch B produced neuroprotective effect on rats subjected to transient focal cerebral ischemia, presumably by inhibiting inflammation and preventing metalloproteinase degradation [31]. Recently, it has been reported that Sch B produced anti-neuroinflammatory action in lipopolysaccharide-induced microglia [32]. Sch B also produced protection against A$\beta_{1\text{-}42}$-induced neurotoxicity *in vitro* [33]. Furthermore, it has recently been reported that Sch B is able to prevent age-related neurodegeneration [34], cerebral ischemia/reperfusion injury *in vivo* [35] and cerebral toxicity induced by hydroperoxide *in vivo* [36].

The tissue non-specific protective action of Sch B has made it a promising lead compound for new drug development. In this regard, *in vivo* pharmacokinetics and tissue distribution study of Sch B has been reported [37]. Sun *et al.* determined the metabolites of Sch B *in vivo* by measuring the accurate mass of the predicted metabolite using Q-TOF [38]. However, there was no precise identification of Sch B metabolites. For a better understanding of the biochemical mechanism underlying the tissue protection afforded by Sch B, we endeavored to investigate the metabolism of Sch B *in vitro* and *in vivo* by MS/MS analyses which enabled the identification of key metabolites.

Mass spectrometry analysis can provide information such as molecular weight, fragment ions and other chemical structural parameters on the analyte. Liquid chromatography coupled with tandem mass spectrometry (LC-MS^n) is a powerful technique for determining and identifying the compound of interest. The high sensitivity of MS used as a LC detector facilitates the detection of new minor constituents, which is otherwise not detectable by classical means. HPLC-MS [39]-[41] and UPLC-MS [42] methods have been used to determine the level of Sch B in biological samples. The results indicated that mass spectrometry was highly specific and sensitive for identifying Sch B from biological matrix. In these studies, LC-MS was proved to be a rapid, specific and sensitive method to detect the presence of Sch B. In the present study, a rapid, sensitive and specific UPLC-MS/MS method was developed to study the *in vitro* and *in vivo* metabolism of Sch B.

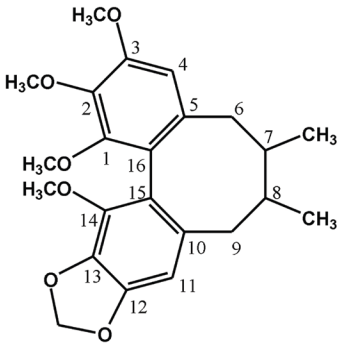

$C_{23}H_{28}O_6$ MW: 400

Figure 1. Chemical structure of schisandrin B.

2. Materials and Methods

2.1. Reagents

Sch B (purity > 99%) was isolated from the fruit of *Schisandra chinensis* (Turcz) Baillon. Rat S9 fraction, NADPH and glucose-6-phosphate (G-6-P) were purchased from Sigma Company (St. Louis, MO, USA). Acetonitrile of HPLC grade was purchased from Duksan Pure Chemicals (Kyunkido, Korea). Methanol was purchased from Tedia (Fairfield, OH, USA). All other reagents were of highest purity available. Potassium phosphate solution is prepared in-house using the aforementioned reagents. Deionized water used in the experiments was produced from a Milli-Q system (Millipore, Milford, MA, USA).

2.2. *In Vitro* Study of Sch B in Rat S9 Fraction

Five microliters of 10 mM Sch B solution was incubated with a 1 mL potassium phosphate solution (100 mM, pH 7.4) containing rat liver S9 fraction (1 mg/mL), cofactors NADPH (1 mM), G-6-P (10 mM) and activator $MgCl_2$ (3 mM). The incubation was carried out for 2 h at 37˚C. The incubation mixture was then collected and 4 mL cold methanol was used to quench the metabolic reaction by precipitating all proteins as well as to extract Sch B and its metabolites. The methanol extract was then centrifuged at 8000 × g for 10 min. The supernatant was dried under nitrogen stream and the residue was dissolved in 3 mL 20% methanol in H_2O (w/w). The reconstituted solution was pretreated by solid phase extraction before the UPLC-MS analysis. Negative control incubations containing no Sch B were conducted under the same experimental conditions, and the samples were also pretreated by solid phase extraction prior to UPLC-MS analysis.

2.3. *In Vivo* Study of the Metabolism of Sch B in Rats

Male Sprague-Dawley rats were obtained from the Animal and Plant Care Facilities in the Hong Kong University of Science & Technology. The experimental protocol was approved by the Research Practice Committee in HKUST. Sch B was orally administered (50 mg/kg) to male Sprague Dawley rats (body weight 200 - 220 g, prior fasting but with water for 12 h). Rats were housed in metabolic cages that allowed the separated collection of urine and feces samples. Urine and feces samples were collected from 0 to 48 hours post-dosing with Sch B.

2.4. Solid Phase Extraction Procedure

All samples from rat liver S9 fraction incubation as well as urine and feces samples were pretreated by solid phase extraction (SPE) prior to UPLC-MS analysis. Waters Sep-Pak C_{18} SPE column (1 mL, 50 mg) was first preconditioned with 2 mL methanol and then equilibrated with 2 mL pure water. Samples were loaded onto the preconditioned SPE columns directly. After being washed with 2 mL pure water, the SPE column was eluted using 2 mL methanol solution. The eluted methanol solution was dried with nitrogen stream, and the residue was reconstituted in 1 mL methanol and centrifuged at 8000 × g for 10 min. The supernatant was injected into the UPLC-MS system for analysis.

2.5. Sample Preparation

Urine samples were filtered and then pretreated by solid phase extraction, as described above. Ten microliter of the supernatant was analyzed by using UPLC-MS and UPLC-MS/MS for Sch B and its metabolites.

Feces samples were suspended in pure water and then the mixture was sonicated for 30 min. The feces suspension was filtered and then pretreated by solid phase extraction. Ten microliter of the supernatant was analyzed by using UPLC-MS and UPLC-MS/MS for Sch B and its metabolites.

2.6. UPLC-ESI-MS Analysis

The UPLC-ESI-MS system consisted of a Waters Acquity ultra performance LC and a Waters Xevo G2 Q-Tof mass spectrometer (Waters, Singapore). Positive ESI ion mode was used to analyze Sch B and its metabolites in biological samples. The following parameters of the mass tune for positive ion mode were used: capillary voltage 3.0 KV, sampling cone 20, extraction cone 4.0, the source temperature at 150˚C and desolvation temperature at 400˚C, the desolvation gas flow at 800 L/h. Full-scan mass spectra at a mass range of *m/z* 50 - 1000 were acquired. Mass chromatogram for protonated molecular $[M + H]^+$ ions of Sch B and its metabolites were used

for the determination. Molecular ion masses of potential metabolites were examined and the corresponding extracted mass chromatograms were recorded. Chromatographic separation was achieved on a Waters Acquity UPLC BEH C_{18} column (2.1 mm × 50 mm, 1.7 μm, Ireland). The mobile phase consisted of 0.1% formic acid in water (A) and acetonitrile (B). The gradient program was from 30% B, changed to 100% B within 2 min and held at 100% B for 4 min, then back to 30% B within 1 min and held 30% B till 10 min at a flow rate of 0.35 mL/min. B. The acquired UPLC-MS data were processed using Marker Lynx (Waters, Singapore).

3. Results

3.1. UPLC-MS and UPLC-MS/MS Analyses of Sch B

Conditions for UPLC and MS analysis were optimized with standard Sch B and the MS chromatogram and MS/MS spectrum of Sch B were shown in **Figure 2**. Sch B was eluted at about 5.27 min under the present

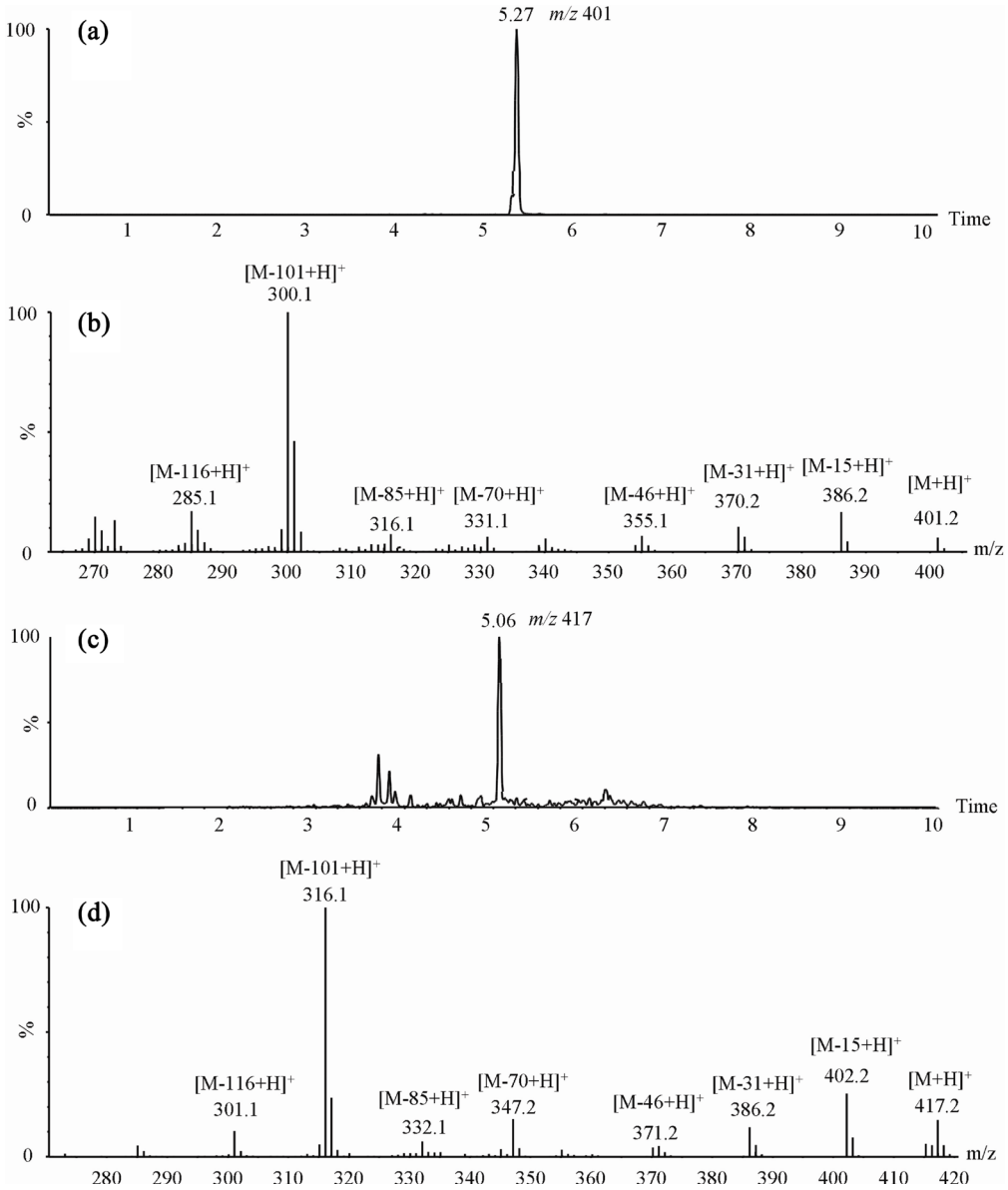

Figure 2. Full scan UPLC-MS chromatogram and MS/MS spectrum of standard Sch B ((a) Raw chromatogram data; (b) MS/MS spectrum) and metabolite M1 ((c) Raw chromatogram data; (d) MS/MS spectrum) detected from the *in vitro* incubation sample with rat S9.

experimental conditions with the protonated molecular ion at *m/z* 401 (**Figure 2(a)**). **Figure 2(b)** shows the MS/MS spectrum of standard Sch B, with the fragment ions at *m/z* 386 (M + H − 15), 370 (M + H − 31), 355 (M + H − 46), 331 (M + H − 70), 316 (M + H − 85), 300 (M + H − 101, base peak) and 285 (M + H − 116).

3.2. Determination of Sch B Metabolites from Rat S9 Fraction Incubation

By comparing with the negative control of *in vitro* incubation, the metabolite detection was achieved by UPLC-MS analysis and confirmed with UPLC-MS/MS experiments in positive ESI mode. One metabolite was detected from the incubation sample, namely, M1. **Figure 2(c)** and **Figure 2(d)** show the UPLC-MS chromatogram and the MS/MS spectrum of the metabolite M1, respectively. The extract ion of M1 was detected at *m/z* 417 (**Figure 2(c)**). **Figure 2(d)** shows the UPLC-MS/MS spectrum of metabolite M1. MS/MS analysis of M1 revealed the same fragment pattern as the parent Sch B (**Figure 2(b)**).

3.3. UPLC-MS/MS Analyses of Metabolites in Feces Collected Sch B-Treated Rats

Similar to the *in vitro* study, the metabolite detections were achieved by UPLC-MS analyses and confirmed with MS/MS experiments in positive ESI mode. After comparing with blank feces sample, four metabolites, namely, M1, M2, M3 and M4 (*m/z* 471, 387, 389 and 565, respectively), were detected in rat feces samples collected during the period of 0 - 48 h following the oral administration of Sch B (**Figure 3**). As shown in **Figure 3(a)**, both UPLC-MS data and MS/MS spectra of the peak at 5.06 (min) were identical to those of M1, whereas the other two peaks at 4.81 and 3.63 were also detected in the blank feces sample. Thus, the peak at 5.06 was identified as M1. Four demethylated metabolites at *m/z* value of 387 were identified at retention times of 4.82, 4.74, 4.68, 3.66 min from the UPLC-MS analysis of the feces sample (**Figure 3(b)**, M2). The peaks at 5.52 and 3.99 also existed in blank feces sample. Three peaks for the extracted ion at *m/z* 389 (M3, **Figure 3(c)**, peak at 3.38 also existed in blank sample) revealed the existence of isomer status for M3. However, the metabolite M4 at *m/z* 565 (M4, **Figure 3(d)**) showed the peak at 3.47.

Figure 4 shows the MS/MS spectrum of M2, M3 and M4. The MS/MS spectra of M2 at 4.82, 4.74, 4.68 and 3.66 in the chromatogram were shown in **Figure 3(b)**. Based on the protonated molecular ion at *m/z* 387 (**Figure 4(a)**), the fragment ions at *m/z* 372, 355 and 340, as well as fragment ions at *m/z* 317, 302, 286 (base peak) and 271 produced a similar fragmentation pattern to that of the parent Sch B (**Figure 2(b)**). While **Figure 4(b)** shows the MS/MS spectrum of M3 at 4.04 and 3.47 in the chromatogram shown in **Figure 3(c)**, **Figure 4(c)** shows the MS/MS spectrum of M4 at 3.47 in the chromatogram shown in **Figure 3(d)**.

3.4. UPLC-MS/MS Analyses of Metabolites in Rat Urine Collected from Sch B-Dosed Rats

Similar to the feces sample, the metabolite detection in urine sample was achieved by UPLC-MS analyses and confirmed with MS/MS experiments in positive ESI mode. When comparing with blank urine sample, three metabolites were detected in rat urine sample collected during the period of 0 - 48 h following the oral administration of Sch B. MS/MS analyses showed that the data were consistent with those of M2-M4, which were identified metabolites in rat feces. UPLC-MS chromatogram and MS/MS spectrum were not described here. The high resolution MS data and accurate MS error of Sch B and the metabolites were shown in **Table 1**. The high accuracy of MS data confirmed the identification of metabolites.

4. Discussion

In the MS/MS spectrum of standard Sch B (**Figure 2(b)**), based on the protonated molecular ion at *m/z* 401, the fragment ions at *m/z* 386 (M + H − 15), 370 (M + H − 31) and 355 (M + H − 46) indicated the loss of CH_3, OCH_3 and OCH_3 + CH_3 moieties, respectively, while the fragment ions at *m/z* 331 (M + H − 70), 316 (M + H − 85), 300 (M + H − 101, base peak) and 285 (M + H − 116) evidenced the loss of C_5H_{10}, C_5H_{10} + CH_3, C_5H_{10} + OCH_3 and C_5H_{10} + OCH_3 + CH_3 moieties, respectively. The results suggested that fragment pathways of Sch B under ESI-MS involved the loss of CH_3 and OCH_3 from the methoxy groups of the structure, as well as opening of the octa-member ring and the loss of C_5H_{10}. The fragment pattern of Sch B, as observed in the present study, was consistent with that reported by He *et al.* [43].

The UPLC-MS chromatogram of metabolite M1 (**Figure 2(c)**) demonstrated that the extract ion of M1 was detected at *m/z* 417 (**Figure 2(c)**), which was 16 Da larger than the parent Sch B (at *m/z* 401) (**Figure 2(a)**),

suggesting that M1 was a mono-oxygenated Sch B. In the UPLC-MS/MS spectrum of metabolite M1 (**Figure 2(d)**), MS/MS analysis of M1 revealed the same fragment pattern as the parent Sch B (**Figure 2(b)**), suggesting that M1 was an oxygenated metabolite of Sch B. The fragment ion at *m/z* 347 $[M - 70 + H]^+$ indicated that the oxygenation site was at C_4 or C_{11}. The identification was further confirmed by high-accuracy MS analysis, with the mass error between the theoretical (417.1913) and measured (417.1923) *m/z* values of the $[M + H]^+$ ion being less than 2.5 ppm (**Table 1**).

Table 1. Molecular formula, accurate mass, measured mass and mass error of Sch B and its metabolites in rat.

Name	Molecular formula	Accurate $[M + H]^+$	Measured $[M + H]^+$	Mass error (ppm)
Sch B	$C_{23}H_{28}O_6$	401.1964	401.1989	6.23
M1	$C_{23}H_{28}O_7$	417.1913	417.1923	2.39
M2	$C_{22}H_{26}O_6$	387.1808	387.1809	0.26
M3	$C_{22}H_{28}O_6$	389.1964	389.1983	4.88
M4	$C_{28}H_{36}O_{12}$	565.2285	565.2281	−0.71

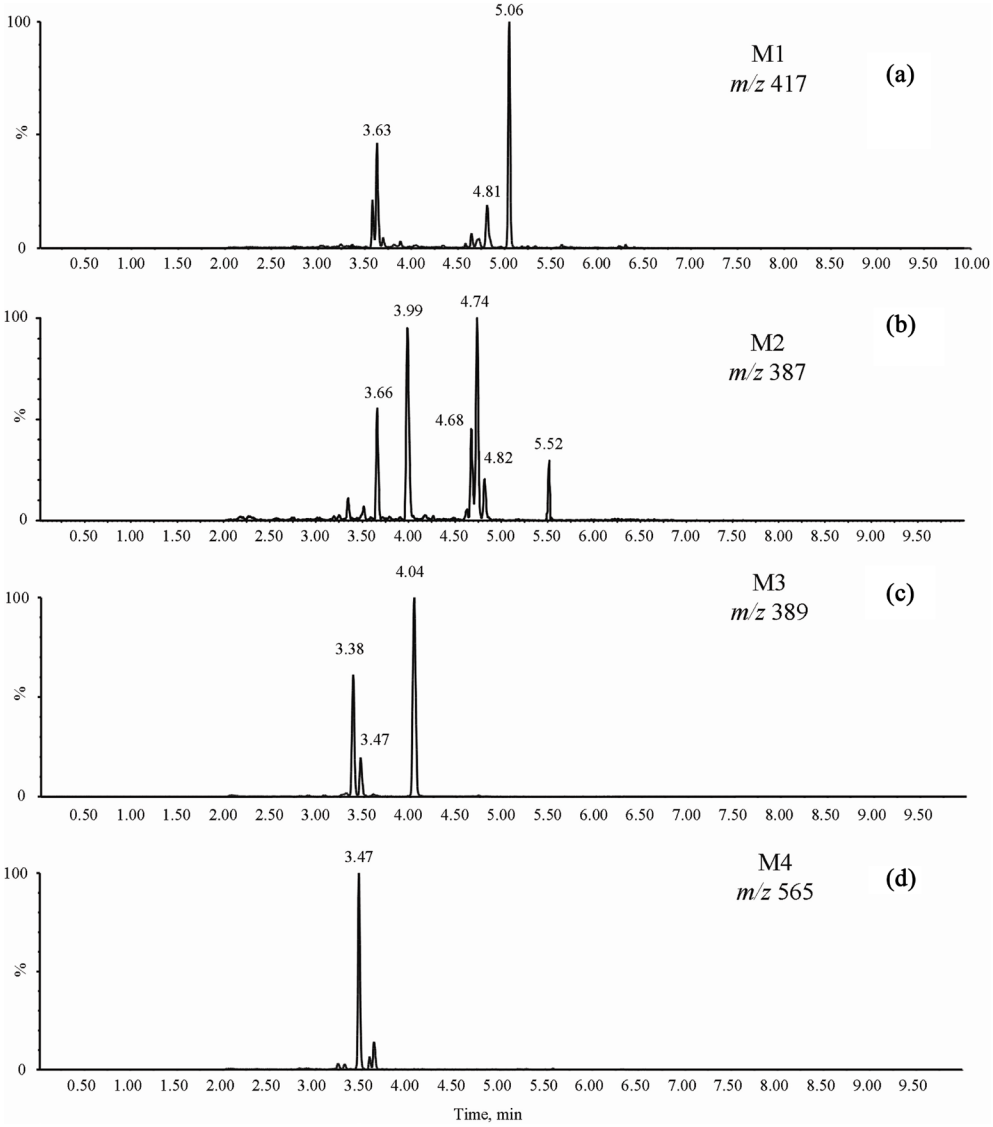

Figure 3. Extracted UPLC-MS chromatogram of M1-M4 *m/z* 417 (a), 387 (b), 389 (c), 565 (d) detected from rat feces sample after oral administration of Sch B.

When we examined the metabolites in feces collected Sch B-treated rats using UPLC-MS/MS four metabolites, namely, M1, M2, M3 and M4, were detected (**Figure 3**). These four isomeric demethylated metabolites (M2, **Figure 3(b)**) may have resulted from the enzymatic hydrolysis of the methoxy groups in Sch B. Three peaks for the extracted ion at *m/z* 389 (M3, **Figure 3(c)**) revealed the existence of isomer status for M3. However, the metabolite M4 at *m/z* 565 (M4, **Figure 3(d)**) showed the peak at 3.47, which was 176 Da larger than the metabolite M3 at *m/z* 389 (**Figure 3(c)**), suggestive of a product derived from the glucuronidation of M3.

The UPLC-MS/MS spectrum of metabolite M2, M3 and M4 were also analyzed in the present study. The MS/MS spectra of M2 (**Figure 4(a)**) at 4.82, 4.74, 4.68 and 3.66 in the chromatogram were shown in **Figure 3(b)**. MS/MS spectra at the four retention times were identical, indicating that four isomeric metabolites existed and their structures were similar, *i.e.* demethylated site was on methoxy groups. Based on the protonated molecular ion at *m/z* 387 (**Figure 4(a)**), the fragment ions at *m/z* 372, 355 and 340, as well as fragment ions at *m/z* 317, 302, 286 (base peak) and 271 produced a similar fragmentation pattern to that of the parent Sch B (**Figure 2(b)**). Thus, M2 was identified as the demethylated Sch B. **Figure 4(b)** shows the MS/MS spectrum of M3 at 4.04

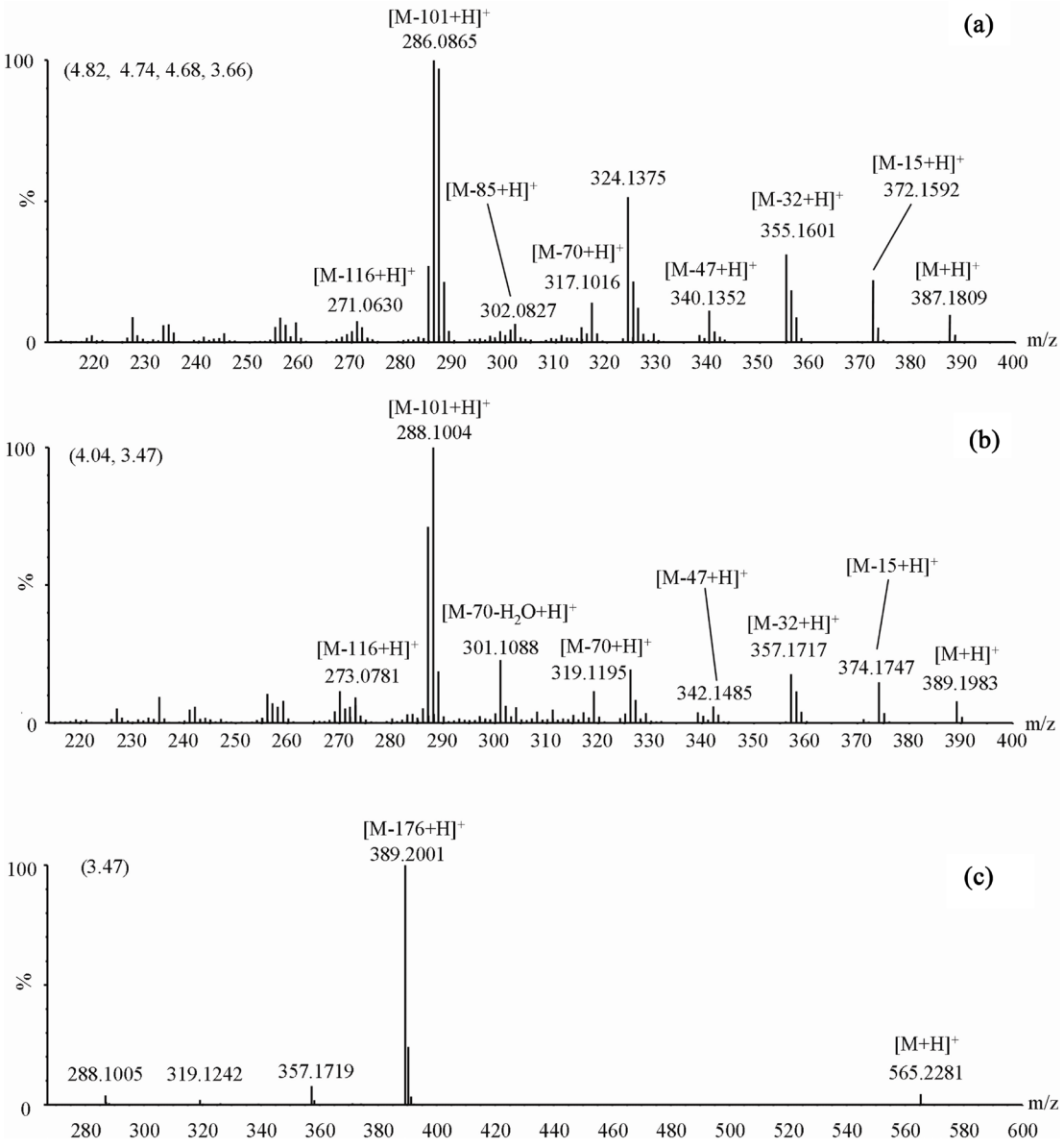

Figure 4. UPLC-MS/MS spectrum of metabolite M2 ((a) Peak at 4.82, 4.74, 4.68 and 3.66 min), M3 ((b) Peak at 4.04 and 3.47 min) and M4 ((c) Peak at 3.47 min).

and 3.47 in the chromatogram shown in **Figure 3(c)**. Similarly, based on the protonated molecular ion at *m/z* 389, the fragment ions at *m/z* 374, 357 and 342, as well as the fragment ions at *m/z* 319, 301, 288 (base peak) and 273 produced a similar fragmentation pattern as the parent Sch B (**Figure 2(b)**), which was identified as the opened five-member ring metabolite of Sch B. **Figure 4(c)** shows the MS/MS spectrum of M4 at 3.47 in the chromatogram shown in **Figure 3(d)**. The fragment ion at *m/z* 389 (base peak) evidenced the loss of 176 Da from the protonated molecular ion at *m/z* 565, other fragment ions were fragmented from the ion at *m/z* 389 and the fragmentation pattern was as same as the metabolite M3. Thus M4 was the glucuronidated form of M3. Conceivably, the peak at 3.47 in **Figure 3(c)** should be M4, which dissociated at ESI source before entered the MS detector. The peak at 4.04 in **Figure 3(c)** should represent M3, which was identified as the opened five-member ring metabolite. Taken together, the metabolic pathway of Sch B in rats was summarized in **Figure 5**.

Results from some recent studies have shed light on the underlying mechanism of how Sch B induces a tissue non-specific antioxidant response [8] [34]. They revealed that the cocomintant production of reactive oxygen species (ROS) during the cytochrome P450 (CYP)-catatlzyed metabolism of Sch B can activate the antioxidant signal transduction pathway with a resultant induction of antioxidant response [8]. However, the metabolite(s) of Sch B which can cause the production ROS is yet to be determined. In the present study, among the four metabolites of Sch B (**Figure 5**), Sch B-M1 was found to possess a catechol moiety. In this connection, some studies also demonstrated that demethylenation of methylendioxy group resulted in the formation of catechol [44]-[46], which is a redox active moiety. Catechol can be oxidized into quinone which undergoes redox cycling and generates ROS [47] [48]. A recent study has also proposed that ROS from quinone redox cycling can elicit antioxidant response via redox signaling [49]. These findings lend a strong support to the involvement of CYP-catalyzed metabolism of the methylenedioxy group in the Sch B molecule in eliciting the antioxidant response and hence tissue protection. An increased understanding the protective mechanism of Sch B has offered a promising prospect of using Sch B as an agent for mitigating the age-related diseases in humans.

5. Conclusion

The method of UPLC coupled to QTOF mass spectrometry was developed and applied to study the metabolic fate of Sch B *in vitro* and *in vivo*. One mono-oxygenated metabolite was found after incubating Sch B with rat S9 fraction *in vitro*. Four metabolites of Sch B were identified from rat feces and urine following the oral

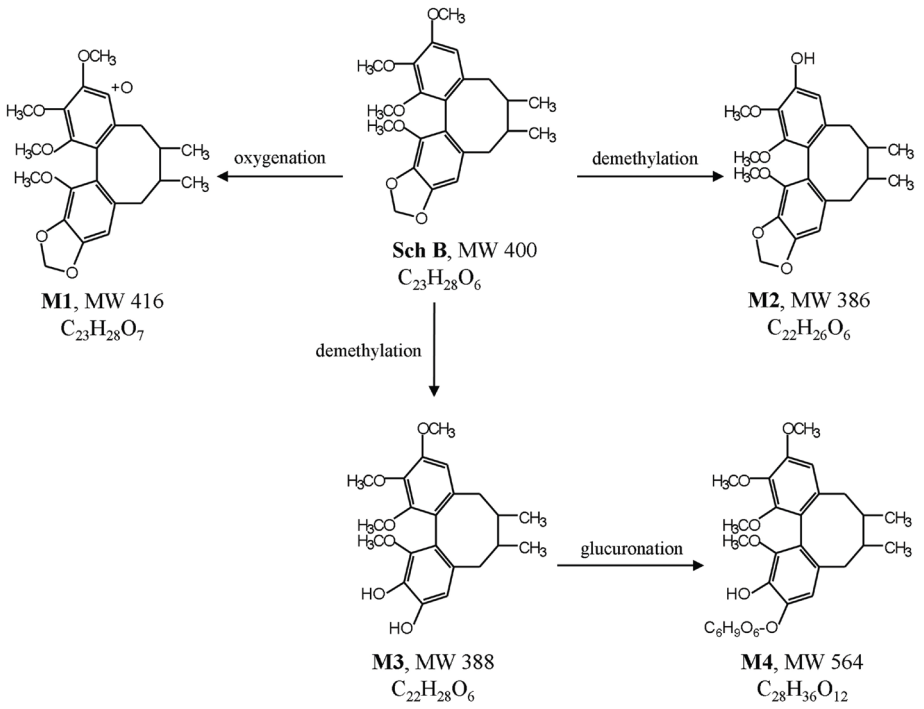

Figure 5. Proposed metabolic pathways of Sch B in rats.

administration of Sch B. The structures of metabolites were elucidated by high-accuracy MS and MS/MS analyses. The metabolic reactions of Sch B were found to mainly involve the mono-oxygenation of C_4 or C_{11}, the demethylation of methoxy groups, the opening of five-member ring and the glucuronidation of metabolites in rats.

Acknowledgements

Dr Wan Chan expresses his sincere thanks the Hong Kong University of Science and Technology for supporting this research (grant R9310). TX Qian was partially supported by a Postdoctoral Fellowship from the Provost office, HKUST.

References

[1] Hancke, J.L., Burgos, R.A. and Ahumada, F. (1999) *Schisandra chinensis*. (Turcz.) Baill. *Fitoterapia*, **70**, 451-471. http://dx.doi.org/10.1016/S0367-326X(99)00102-1

[2] Balandin, D.A. (1951) Schizandrin—A New Stimulant from Schizandra Fruits. In: Lazarev, N.V., Ed., *Materials for the Study of Stimulants and Tonics from Ginseng and Schizandra Roots*, Far East Branch of USSR Academy of Science, Vladivotok, 45-50.

[3] Liu, X., Zhang, C., Jin, X., Li, Y., Zheng, X. and Li, L. (2007) Inhibitory Effect of Schisandrin B on Gastric Cancer Cells *in Vitro*. *World Journal of Gastroenterology*, **13**, 6506-6511. http://dx.doi.org/10.3748/wjg.13.6506

[4] Li, L., Lu, Q., Shen, Y. and Hu, X. (2006) Schisandrin B Enhances Doxorubicin-Induced Apoptosis of Cancer Cells but Not Normal Cells. *Biochemical Pharmacology*, **71**, 584-595. http://dx.doi.org/10.1016/j.bcp.2005.11.026

[5] Li, L., Wang, T., Xu, Z., Yu, Y., Chen, W. and Chen, F. (2005) Effects of Schisandrin B on Reversing Multidrug Resistance in Human Breast Cancer Cells Transfected with mdr1 Gene. *Chinese Medical Journal*, **85**, 1633-1637.

[6] Xu, Y., Liu, Z., Sun, J., Pan, Q., Sun, F., Yan, Z. and Hu, X. (2011) Schisandrin B Prevents Doxorubicin-Induced Chronic Cardiotoxicity and Enhances Its Anticancer Activity *in Vivo*. *PLoS ONE*, **6**, e28335. http://dx.doi.org/10.1371/journal.pone.0028335

[7] Chen, Y., Ip, S.P., Ko, K.M., Poon, T.C., Ng, E.W., Lai, P,B., Mao, Q.Q., Xian, Y.F. and Che, C.T. (2011) A Proteomic Approach in Investigating the Hepatoprotective Mechanism of Schisandrin B: Role of Raf Kinase Inhibitor Protein. *Journal of Proteome Research*, **10**, 299-304. http://dx.doi.org/10.1021/pr100871h

[8] Leong, P.K., Chiu, P.Y., Leung, H.Y. and Ko, K.M. (2012) Cytochrome P450-Catalysed Reactive Oxygen Species Production Mediates the (−)Schisandrin B-Induced Glutathione and Heat Shock Responses in AML12 Hepatocytes. *Cell Biology International*, **36**, 321-326. http://dx.doi.org/10.1042/CBI20090451

[9] Pu, H.J., Cao, Y.F., He, R.R., Zhao, Z.L., Song, J.H., Jiang, B., Huang, T., Tang, S.H., Lu, J.M. and Kurihara, H. (2012) Correlation between Antistress and Hepatoprotective Effects of Schisandra Lignans Was Related with Its Antioxidative Actions in Liver Cells. *Evidence-Based Complementary and Alternative Medicine*, **2012**, Article ID: 161062. http://dx.doi.org/10.1155/2012/161062

[10] Chiu, P.Y., Leung, H.Y., Siu, A.H., Poon, M.K. and Ko, K.M. (2007) Schisandrin B Decreases the Sensitivity of Mitochondria to Calcium Ion-Induced Permeability Transition and Protects against Carbon Tetrachloride Toxicity in Mouse Livers. *Biological and Pharmaceutical Bulletin*, **30**, 1108-1112. http://dx.doi.org/10.1248/bpb.30.1108

[11] Pan, S.Y., Han, Y.F., Carlier, P.R., Pang, Y.P., Mak, D.H., Lam, B.Y. and Ko, K.M. (2002) Schisandrin B Protects against Tacrine- and Bis(7)-Tacrine-Induced Hepatotoxicity and Enhances Cognitive Function in Mice. *Planta Medica*, **68**, 217-220. http://dx.doi.org/10.1055/s-2002-23145

[12] Chiu, P.Y., Tang, M.H. and Ko, K.M. (2003) Hepatoprotective Mechanism of Schisandrin B: Role of Mitochondrial Glutathione Antioxidant Status and Heat Shock Proteins. *Free Radical Biology and Medicine*, **35**, 368-380. http://dx.doi.org/10.1016/S0891-5849(03)00274-0

[13] Stacchiotti, A., Volti, G.L. and Rodella, L.F. (2009) Schisandrin B Stimulates a Cytoprotective Response in Rat Liver Exposed to Mercuric Chloride. *Food and Chemical Toxicology*, **47**, 2834-2840. http://dx.doi.org/10.1016/j.fct.2009.09.003

[14] Li, L., Zhang, T., Zhou, L., Xing, G., Chen, Y. and Xin, Y. (2013) Schisandrin B Attenuates Acetaminophen-Induced Hepatic Injury through Overexpression of Heat Shock Protein 27 and 70 in Mice. *Journal of Gastroenterology and Hepatology*, **23**, 640-647.

[15] Pan, S.Y., Jia, Z.H., Zhang, Y., Yu, Q., Wang, X.Y., Sun, N., Zhu, P.L., Yu, Z.L. and Ko, K.M. (2013) A Novel Mouse Model of Combined Hyperlipidemia Associated with Steatosis and Liver Injury by a Single-Dose Intragastric Administration of Schisandrin B/Cholesterol/Bile Salts Mixture. *Journal of Pharmacological Sciences*, **123**, 110-119. http://dx.doi.org/10.1254/jphs.13087FP

[16] Pao, T.T., Hsu, K.F., Liu, K.T., Chang, L.G., Chuang, C.H. and Sung, C.Y. (1977) Protective Action of Schizandrin B on Hepatic Injury in Mice. *Chinese Medical Journal* (*English Edition*), **3**, 173-179.

[17] Bunel, V., Antoine, M.H., Nortier, J., Duez, P. and Stévigny, C. (2013) Protective Effects of Schizandrin and Schizandrin B towards Cisplatin Nephrotoxicity *in Vitro*. *Journal of Applied Toxicology*, **34**, 1311-1319. http://dx.doi.org/10.1002/jat.2951

[18] Li, M., Jin, J., Li, J., Guan, C.W., Wang, W.W., Qiu, Y.W. and Huang, Z.Y. (2012) Schisandrin B Protects against Nephrotoxicity Induced by Cisplatin in HK-2 Cells via Nrf2-ARE Activation. *Acta Pharmaceutica Sinica*, **47**, 1434-1439.

[19] Zhu, S., Wang, Y., Chen, M., Jin, J., Qiu, Y., Huang, M. and Huang, Z. (2012) Protective Effect of Schisandrin B against Cyclosporine A-Induced Nephrotoxicity *in Vitro* and *in Vivo*. *The American Journal of Chinese Medicine*, **40**, 551-566. http://dx.doi.org/10.1142/S0192415X12500425

[20] Chiu, P.Y., Leung, H.Y. and Ko, K.M. (2008) Schisandrin B Enhances Renal Mitochondrial Antioxidant Status, Functional and Structural Integrity, and Protects against Gentamicin-Induced Nephrotoxicity in Rats. *Biological and Pharmaceutical Bulletin*, **31**, 602-605. http://dx.doi.org/10.1248/bpb.31.602

[21] Stacchiotti, A., Volti, G., Lavazza, A., Schena, I., Aleo, M.F., Rodella, L.F. and Rezzani, R. (2011) Different Role of Schisandrin B on Mercury-Induced Renal Damage *in Vivo* and *in Vitro*. *Toxicology*, **286**, 48-57. http://dx.doi.org/10.1016/j.tox.2011.05.005

[22] Liu, W., Xu, Z., Yang, H., Deng, Y., Xu, B. and Wei, U. (2011) The Protective Effects of Tea Polyphenols and Schisandrin B on Nephrotoxicity of Mercury. *Biological Trace Element Research*, **143**, 1651-1665. http://dx.doi.org/10.1007/s12011-011-8996-y

[23] Chiu, P.Y., Lam, P.Y., Yan, C.W. and Ko, K.M. (2011) Schisandrin B Protects against Solar Irradiation-Induced Oxidative Injury in BJ Human Fibroblasts. *Fitoterapia*, **82**, 682-691. http://dx.doi.org/10.1016/j.fitote.2011.02.010

[24] Ip, S.P. and Ko, K.M. (1996) The Crucial Antioxidant Action of Schisandrin B in Protecting against Carbon Tetrachloride Hepatotoxicity in Mice: A Comparative Study with Butylated Hydroxytoluene. *Biochemical Pharmacology*, **52**, 1687-1693. http://dx.doi.org/10.1016/S0006-2952(96)00517-5

[25] Xue, J., Liu, G., Wei, H. and Pan, Y. (1992) Antioxidant Activity of Two Dibenzocyclooctene Lignans on the Aged and Ischemic Brain in Rats. *Free Radical Biology and Medicine*, **12**, 127-135. http://dx.doi.org/10.1016/0891-5849(92)90006-3

[26] Zhang, T.M., Wang, B.E. and Liu, G.T. (1989) Action of Schizandrin B, an Antioxidant, on Lipid Peroxidation in Primary Cultured Hepatocytes. *Acta Pharmacologica Sinica*, **10**, 353-356. (Article in Chinese)

[27] Giridharan, V.V., Thandavarayan, R.A., Sato, S., Ko, K.M. and Konishi, T. (2011) Prevention of Scopolamine-Induced Memory Deficits by Schisandrin B, an Antioxidant Lignan from *Schisandra chinensis* in Mice. *Free Radical Research*, **45**, 950-958. http://dx.doi.org/10.3109/10715762.2011.571682

[28] Lam, P.Y., Yan, C.W. and Ko, K.M. (2011) Schisandrin B Protects against Solar Irradiation-Induced Oxidative Stress in Rat Skin Tissue. *Fitoterapia*, **82**, 393-400. http://dx.doi.org/10.1016/j.fitote.2010.11.018

[29] Checker, R., Patwardhan, R.S. and Sandur, S.K. (2012) Schisandrin B Exhibits Anti-Inflammatory Activity through Modulation of the Redox-Sensitive Transcription Factors Nrf2 and NF-kB. *Free Radical Biology and Medicine*, **53**, 1421-1430. http://dx.doi.org/10.1016/j.freeradbiomed.2012.08.006

[30] Lam, P.Y. and Ko, K.M. (2012) Beneficial Effect of (-)Schisandrin B against 3-Nitropropionic Acid-Induced Cell Death in PC12 Cells. *Biofactors*, **38**, 219-225. http://dx.doi.org/10.1002/biof.1009

[31] Lee, T.H., Jung, C.H. and Lee, D.H. (2012) Neuroprotective Effects of Schisandrin B against Transient Focal Cerebral Ischemia in Sprague-Dawley Rats. *Food and Chemical Toxicology*, **50**, 4239-4245. http://dx.doi.org/10.1016/j.fct.2012.08.047

[32] Zeng, K., Zhang, T., Fu, H., Liu, G. and Wang, X. (2012) Schisandrin B Exerts Anti-Neuroinflammatory Activity by Inhibiting the Toll-Like Receptor 4-Dependent MyD88/IKK/NF-κB Signaling Pathway in Lipopolysaccharide-Induced Microglia. *European Journal of Pharmacology*, **692**, 29-37. http://dx.doi.org/10.1016/j.ejphar.2012.05.030

[33] Wang, B. and Wang, X. (2009) Schisandrin B Protects Rat Cortical Neurons against Abeta1-42-Induced Neurotoxicity. *Pharmazie*, **64**, 450-454.

[34] Lam, P.Y. and Ko, K.M. (2012) Schisandrin B as a Hormetic Agent for Preventing Age-Related Neurodegenerative Diseases. *Oxidative Medicine and Cellular Longevity*, **2012**, Article ID: 250825. http://dx.doi.org/10.1155/2012/250825

[35] Chen, N., Chiu, P.Y. and Ko, K.M. (2008) Schisandrin B Enhances Cerebral Mitochondrial Antioxidant Status and Structural Integrity, and Protects against Cerebral Ischemia/Reperfusion Injury in Rats. *Biological and Pharmaceutical Bulletin*, **31**, 1387-1391. http://dx.doi.org/10.1248/bpb.31.1387

[36] Ko, K.M. and Lam, B.Y. (2002) Schisandrin B Protects against Tert-Butylhydroperoxide Induced Cerebral Toxicity by Enhancing Glutathione Antioxidant Status in Mouse Brain. *Molecular and Cellular Biochemistry*, **238**, 181-186. http://dx.doi.org/10.1023/A:1019907316129

[37] Zhu, H., Zhang, X., Guan, J., Cui, B., Zhao, L. and Zhao, X. (2013) Pharmacokinetics and Tissue Distribution Study of Schisandrin B in Rats by Ultra-Fast Liquid Chromatography with Tandem Mass Spectrometry. *Journal of Pharmaceutical and Biomedical Analysis*, **78-79**, 136-140. http://dx.doi.org/10.1016/j.jpba.2013.01.041

[38] Sun, H., Wu, F., Zhang, A., Wei, W., Han, Y. and Wang, X. (2013) Profiling and Identification of the Absorbed Constituents and Metabolites of *Schisandra* Lignans by Ultra-Performance Liquid Chromatography Coupled to Mass Spectrometry. *Biomedical Chromatography*, **27**, 1511-1519. http://dx.doi.org/10.1002/bmc.2951

[39] Wang, B.L., Hu, J.P. and Li, Y. (2008) Simultaneous Quantification of Four Active *Schisandra* Lignans from a Traditional Chinese Medicine *Schisandra chinensis* (Wuweizi) in Rat Plasma Using Liquid Chromatography/Mass Spectrometry. *Journal of Chromatography B*, **865**, 114-120. http://dx.doi.org/10.1016/j.jchromb.2008.02.016

[40] Huang, X., Song, F., Liu, Z. and Liu, S. (2007) Studies on Lignan Constituents from *Schisandra chinensis* (Turcz.) Baill. Fruits Using High-Performance Liquid Chromatography/Electrospray Ionization Multiple-Stage Tandem Mass Spectrometry. *Journal of Mass Spectrometry*, **42**, 1148-1161. http://dx.doi.org/10.1002/jms.1246

[41] Tang, J., Shao, B., Liu, Y., Liu, H., Ji, H., Zhu, D. and Wu, L. (2010) Highly Sensitive Determination of Schisandrin and Schisandrin B in Plasma of Rats after Administration of Wurenchun (Fructus Schisandrae Chinensis Extracts) Preparations by LC-ESI-MS/MS. *Biomedical Chromatography*, **24**, 675-681.

[42] Sun, H., Wu, F., Zhang, A., Wei, W., Han, Y. and Wang, X. (2013) Pharmacokinetic Study of Schisandrin, Schisandrol B, Schisantherin A, Deoxyschisandrin, and Schisandrin B in Rat Plasma after Oral Administration of Shengmaisan Formula by UPLC-MS. *Journal of Separation Science*, **36**, 485-491. http://dx.doi.org/10.1002/jssc.201200887

[43] He, R., Tan, P., Han, J., Lin, H., Chen, X., Liu, Y. and Zhang, Y. (2013) ESI/MS Study on Fragmentation Pathways of Schisandrin B by the Discovery Studio, World Science and Technology/Modernization of Traditional Chinese Medicine and Materia. *Medica*, **15**, 527-530.

[44] Corveia, M.A. and Montellauo, P.O. (2005) Inhibition of Cytochrome P450 Enzymes. In: Ortiz de Montellano, P.R., Ed., *Cytochrome P*450: *Structure, Mechanism and Biochemistry*, Kluwer Academic, New York, 263-365.

[45] Iwata, H., Tezuka, Y., Kadota, S., Hiratsuka, A. and Watabe, T. (2004) Identification and Characterization of Potent CYP3A4 Inhibitors in Schisandra Fruit Extract. *Drug Metabolism and Disposition*, **32**, 1351-1358. http://dx.doi.org/10.1124/dmd.104.000646

[46] Donato, M.T. and Castell, J.V. (2003) Strategies and Molecular Probes to Investigate the Role of Cytochrome P450 in Drug Metabolism: Focus on *in Vitro* Studies. *Clinical Pharmacokinetics*, **42**, 153-178. http://dx.doi.org/10.2165/00003088-200342020-00004

[47] Erlank, H., Elmann, A., Kohen, R. and Kanner, J. (2011) Polyphenols Activate Nrf2 in Astrocytes via H_2O_2, Semiquinones, and Quinones. *Free Radical Biology and Medicine*, **51**, 2319-2327. http://dx.doi.org/10.1016/j.freeradbiomed.2011.09.033

[48] Rubiolo, J.A., Mithieux, G. and Vega, F.V. (2008) Resveratrol Protects Primary Rat Hepatocytes against Oxidative Stress Damage: Activation of the Nrf2 Transcription Factor and Augmented Activities of Antioxidant Enzymes. *European Journal of Pharmacology*, **591**, 66-72. http://dx.doi.org/10.1016/j.ejphar.2008.06.067

[49] D'Autreaux, B. and Toledano, M.B. (2007) ROS as Signalling Molecules: Mechanisms That Generate Specificity in ROS Homeostasis. *Nature Reviews Molecular Cell Biology*, **8**, 813-324. http://dx.doi.org/10.1038/nrm2256